Novel Tensor Transform-Based Method of Image Reconstruction From Limited-Angle Projection Data

Artyom M. Grigoryan and Nan Du

Department of Electrical and Computer Engineering
University of Texas at San Antonio

Outline

- Abstract
- Introduction
- Problem Formulation and Methodology
  - Image Model and Line-integrals
  - Image and Splitting-signals
  - Incomplete Set of Projections
  - Ray-integrals and Ray-sums
- Preliminary Results
- Conclusion and Future Work
- References

Abstract

The tensor representation is an effective way to reconstruct the image from a finite number of projections, especially, when projections are limited in a small range of angles. The image is considered in the image plane and reconstruction is in the Cartesian lattice.

This paper introduces a new approach for calculating the splitting-signals of the tensor transform of the discrete image $f(x_i, y_j)$ from a fine number of ray-integrals of the real image $f(x,y)$. The properties of the tensor transform allows for calculating a large part of the 2-D discrete Fourier transform in the Cartesian lattice and obtain high quality reconstructions, even when using a small range of projections, such as [0, 30°) and down to [0, 20°). The experimental results show that the proposed method reconstructs images more accurately than the known method of convex projections and filtered back-projection.

Introduction

- Image Reconstruction

Image reconstruction from projections is a mathematical process of producing an image of two-dimensional distribution (usually of some physical property) from estimates of its line-integrals along a finite number of lines of known locations.

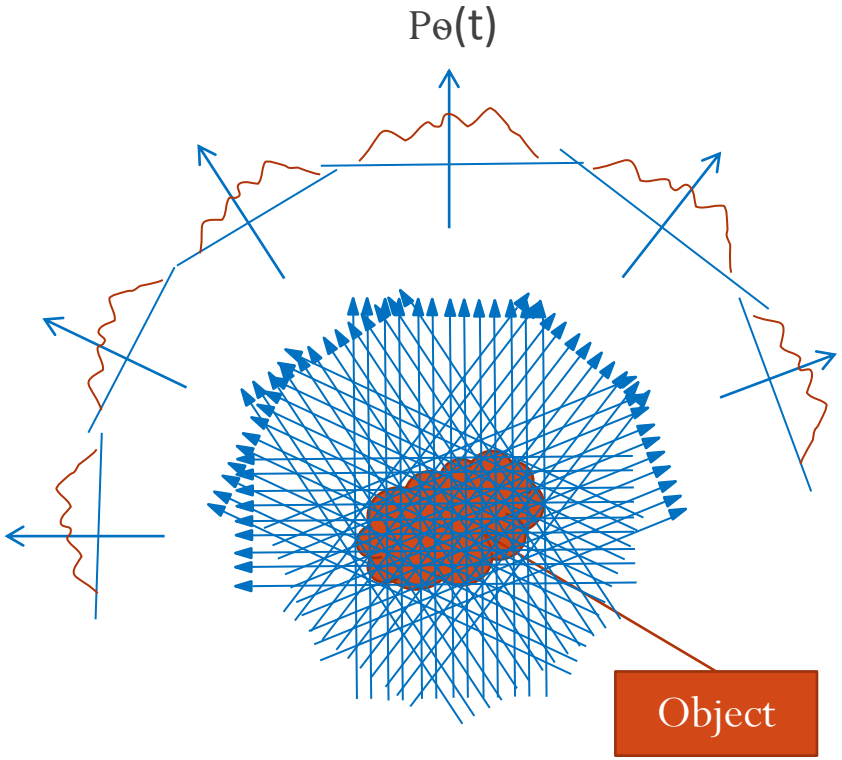

- Limited-angle tomography
  - Not possible to collect projection data over a complete angular range of 180º.
  - Digital breast tomosynthesis, dental tomography, electron microscopy, etc.
  - Reducing: scanning time, patient dose.

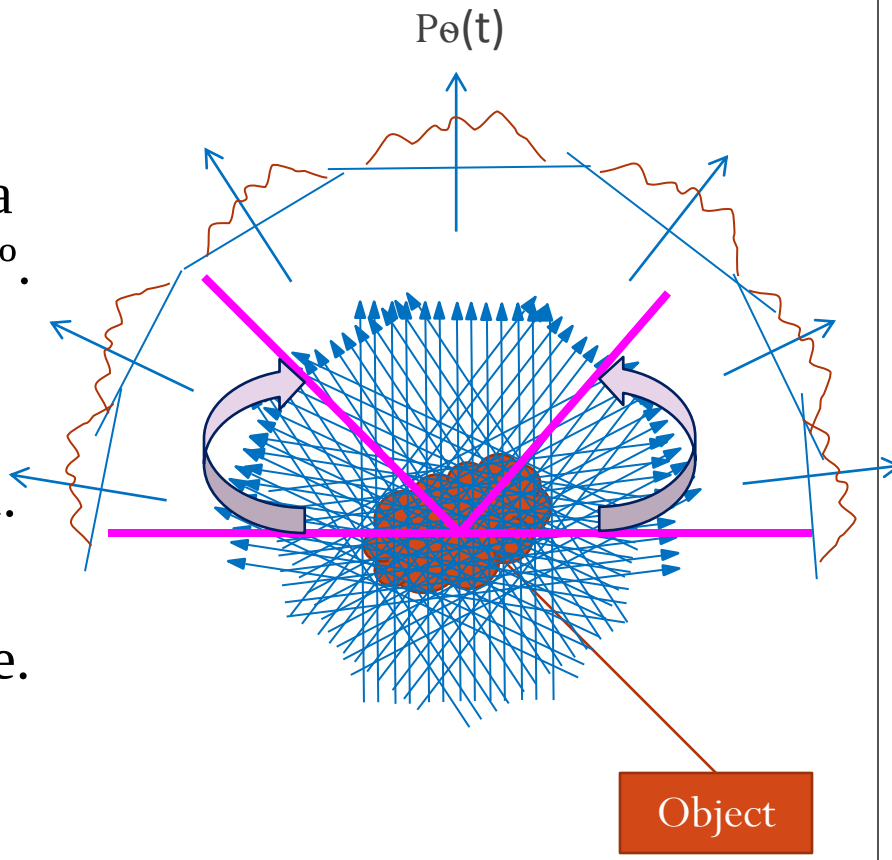

Analytical Reconstruction

- The mathematical problem of determination of functions $f(x, y)$ from an infinite set of their line-integrals(projections) was solved by Radon in 1917.

$$(R \circ \bar{f})(l,\theta) = \int_{-\infty}^{+\infty} \bar{f}(\sqrt{l^2+z^2}, \theta - \arctan(\frac{z}{l}))\, dz \quad \text{If } l \neq 0$$

$$(R \circ \bar{f})(0,\theta) = \int_{-\infty}^{+\infty} \bar{f}(z, \theta - \frac{\pi}{2})\, dz \quad \text{If } l = 0$$

$$R(l,\theta) \rightarrow \bar{f}(r,\phi) = f(x,y)$$

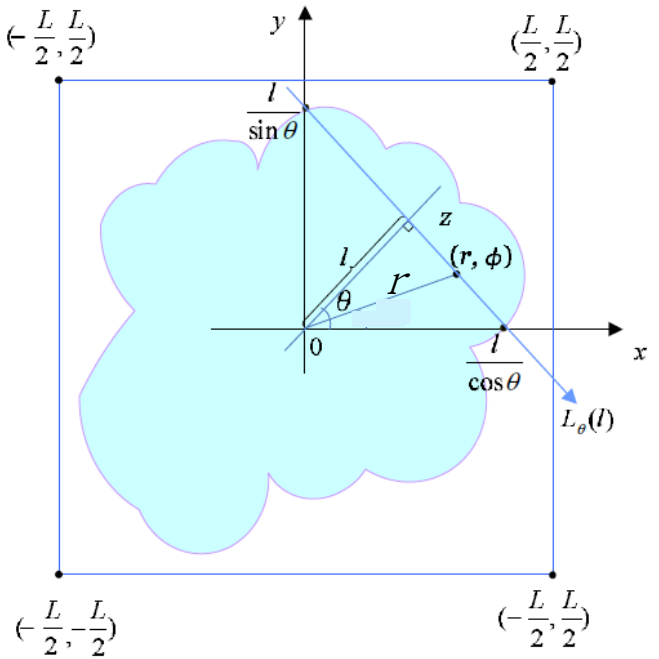

Figure 1. The geometry of projection by angle -($\pi/2$-θ) to the horizontal line.

Sampled version of the inverse Radon transform

- Adapt Radon's fundamental theory to the discrete model.
- The results are approximated and erroneous.

- The main formula obtained in computerized tomography allow us to express the image in the form of the Fourier slice theorem.

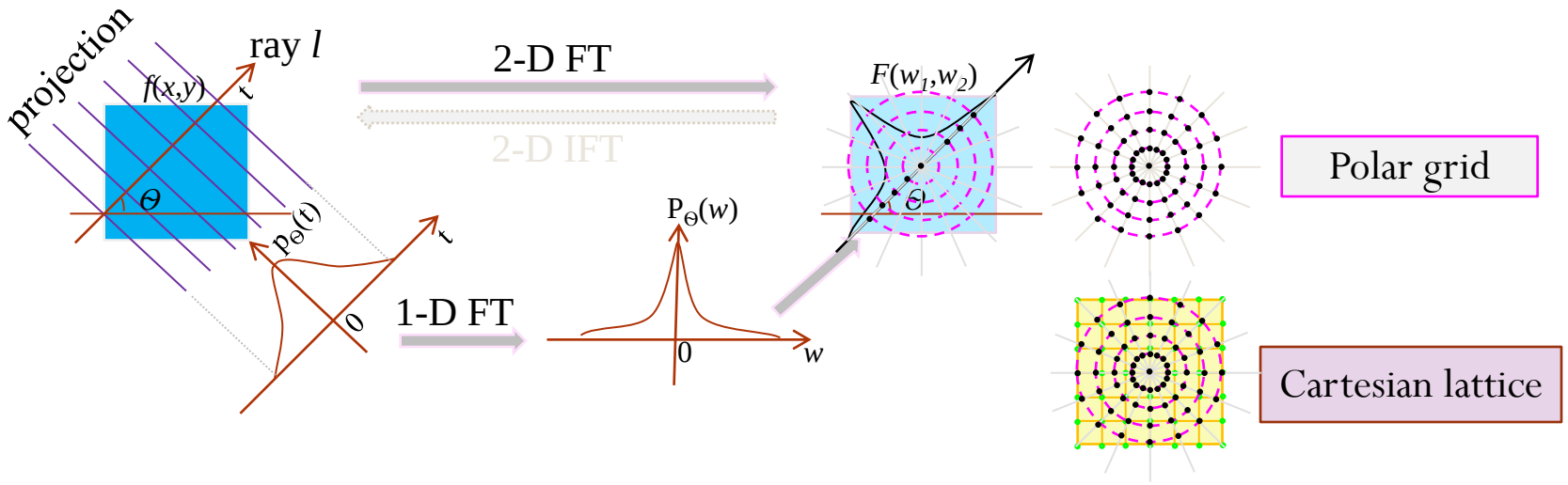

Figure 2. Diagram of Fourier slice theorem.

- **Methods based on the Fourier slice theorem**
  - Interpolation is required
  - Filtered back-projection (FBP) methods
  - Computational efficiency and numerical stability
  - Reconstructions are not exact but approximations of the discrete images

- **Tensor-transform based method**
  - Based on the tensor representation of a two-dimensional image with respect to the Fourier transform.
  - Defines image as a set of one-dimensional(1-D) signals that split the Fourier transform into a set of 1-D transforms.

- Proposed method

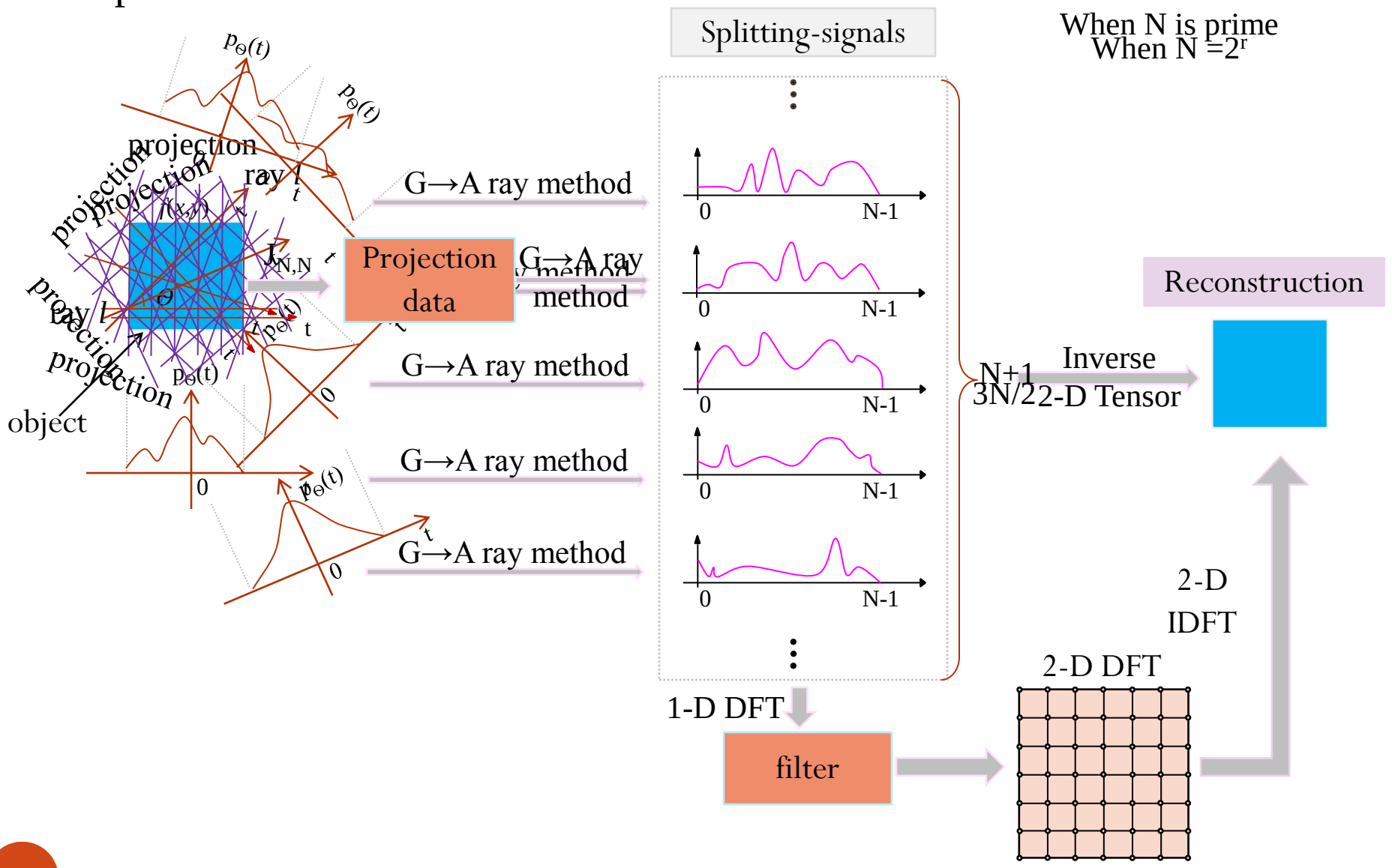

Image Model and Line-integrals

- The image $f(x,y)$ is considered in the discrete form $f_d(x,y)$ which has constant values inside small pieces or image elements (IE) of size $(\Delta x)\times(\Delta y)$ each,

$$f_d(x,y) = \frac{1}{(\Delta x)^2}\int_{IE} f(x,y)dxdy \ , \ \text{if} \ \ (x,y)\in IE.$$

- The image can be considered in the matrix form

$$f(n,m) = \int_{(n,m)-th\ IE} f(x,y)dxdy = (\Delta x)^2 f_d(x_0,y_0),$$

$$(x_0,y_0)\in (n,m)-th\ IE.$$

- The discrete image is considered on the square grid $X_{N,N} = \{(n,m);\ n,m = 0:N-1\}$ inside the region $[0,1]\times[0,1]$.

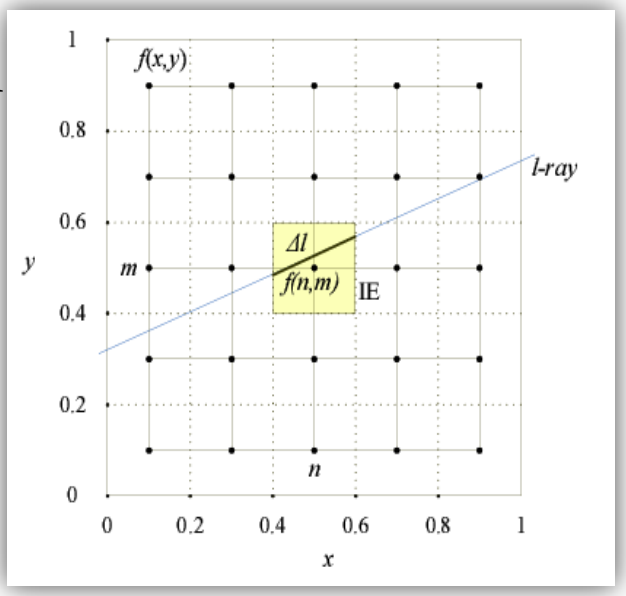

Figure 3. Model of the Image on the 5x5 grid

- The line-integral along a ray l in the (n,m)-th IE is

$$w_l^{(n,m)} = \int_{(n,m)-th\ IE} f(x,y)dl = (\Delta l) f_d(x_0, y_0) = (\Delta l) N^2 f_{n,m}.$$

where $\Delta l = \Delta l_{n,m}$ is the length of the ray l in the (n,m)-th IE.

$$f_{n,m} = \frac{1}{(\Delta l_{n,m}) N^2} w_l^{(n,m)}, \quad n,m = 0:N-1$$

- The line-sum of the discrete image along the same ray is

$$v_l = \sum_{(n,m)\in l} f_{n,m} = \frac{1}{N^2} \sum_{(n,m)\in l} \frac{1}{\Delta l_{n,m}} w_l^{(n,m)}.$$

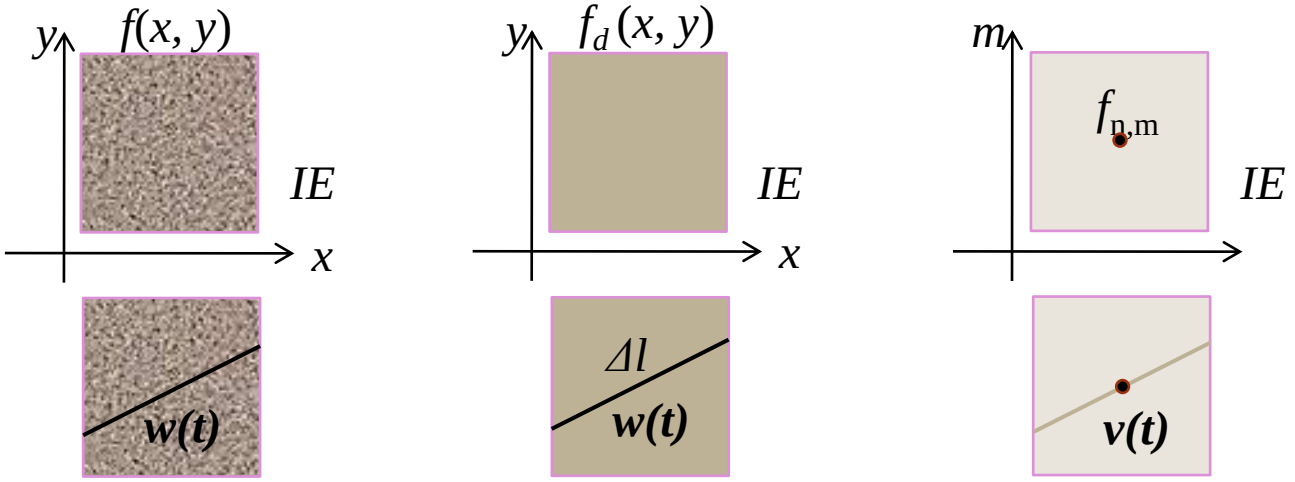

Image and Splitting-signals

- The tensor representation of the image $f_{n,m}$ of size $N \times N$ is defined as a set of splitting-signal of length N.

$$\chi : \{ f_{n,m} \} \to \left\{ f_{T_{p,s}} = \{ f_{p,s,t}; t = 0 : (N-1) \} \right\}_{(p,s) \in J_{N,N}}$$

  - The components of these signals are calculated as the sum of the image along parallel lines.

$$f_{p,s,t} = \sum_{n,m} \{ f_{n,m}; np + ms = t \bmod N \}$$

  - The cyclic group is defined as

$$T_{p,s} = \{ (kp \bmod N, ks \bmod N); k = 0 : (N-1) \}$$

- One can construct different sets $J_{N,N}$, however, their cardinalities are equal.

$$J_{4,4} = \{(1,0),(1,1),(1,2),(1,3),(0,1),(2,1)\},$$

$$J_{5,5} = \{(1,0),(1,1),(1,2),(1,3),(1,4),(0,1)\}.$$

or

$$J_{4,4} = \{(0,1),(1,1),(2,1),(3,1),(1,0),(1,2)\},$$

$$J_{5,5} = \{(0,1),(1,1),(2,1),(3,1),(4,1),(1,0)\}.$$

- In general, we consider

(L+1) generators

$$J_{L,L} = \{(1,0),(1,1),(1,2),\ldots,(1,L-1)\} \cup \{(0,1)\},$$

$$J_{2^r,2^r} = \{(1,0),(1,1),(1,2),\ldots,(1,2^r-1)\} \cup \{(0,1),(2,1),\ldots(2^r-2,1)\}.$$

$3(2^{r-1})$ generators

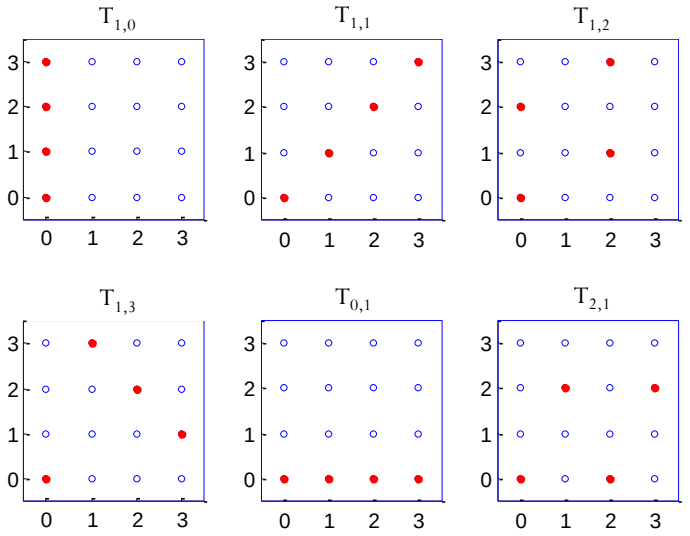

Figure 4. Irreducible covering $\sigma_{4,4}$.

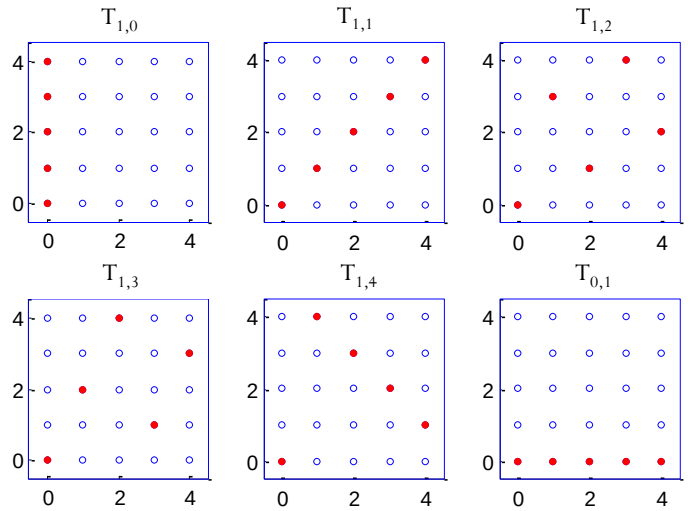

Figure 5. Irreducible covering $\sigma_{5,5}$

- The value of the 2-D DFT of the image at frequency-points of the group *Tp,s:*

$$F_{kp \bmod N,\, ks \bmod N} = \sum_{t=0}^{N-1} f_{p,s,t} W^{kt}, \quad k = 0 : (N-1)$$

where $W=W_N=\exp(-2\pi j/N)$.

The image $f_{n,m}$ of size N×N, where N is a power of 2, can be composed splitting-signals as follows:

$$f_{n,m} = \frac{1}{2N} \sum_{k=0}^{r-1} \frac{1}{2^k} \sum_{(p,s) \in J_{N/2^k, N/2^k}} [\, f_{2^k p, 2^k s, t} - f_{2^k p, 2^k s, t+N/2} \,] + \frac{1}{N^2} f_{0,0,0}$$

where we denote $t = t(2^k p, 2^k s; n, m) = (n2^k p, m2^k s) \bmod N$. All components $f_{2^k p, 2^k s, t}$ in this equation can be calculated using the following recursive formula:

$$f_{2^k p, 2^k s, t_1} = f_{2^{k-1} p, 2^{k-1} s, 2^{k-1} t_1} + f_{2^{k-1} p, 2^{k-1} s, 2^{k-1} t_1 + N/2}, \quad k = 1, 2, \ldots, r-1,$$

where p or s equals 1, and $t_1 = 0 : (N/2^{k+1} - 1)$.

- In other words, these components can be calculated from 3N/2 splitting-signals $f_{Tp,s}$ generated by the frequencies (p, s).

$$d_{n,m} = f_{p,s,(np+ms) \bmod N}, \qquad n,m = 0 : (N-1),$$

- Each image is the direction image with N values of the splitting-signal $f_{Tp,s}$, which are located along the parallel lines (np +ms) mod N, which pass through the knots of the lattice.

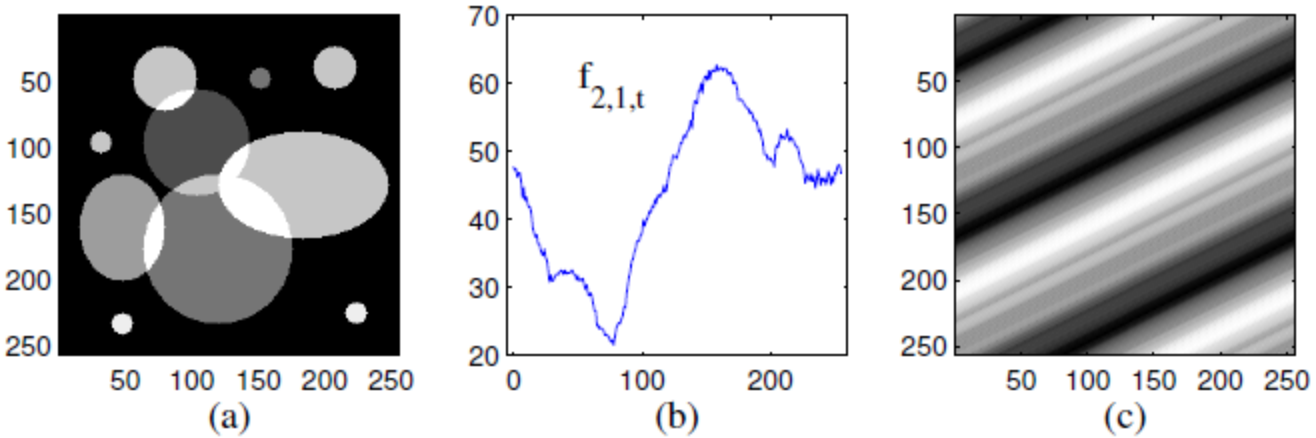

Figure 6. (a) The 256×256 image, (b) splitting-signal $\{f_{2,1,t}; t=0:255\}$, and (c) the corresponding direction image.

Incomplete Set of Projections

- Equivalent sets of angles

The complete set of angles: $\Phi_N = \{\arctan(s/p);(p,s) \in J_{N,N}\}$

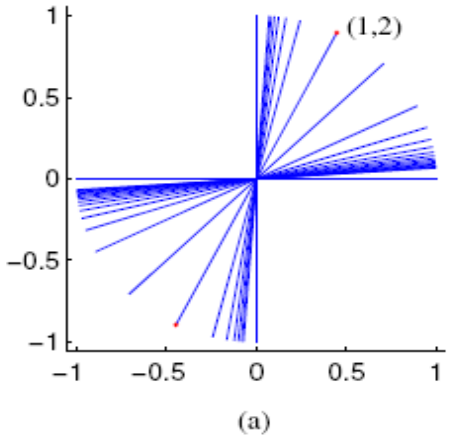

(a)

$J_{16,16}$

$$J_{N,N} = \{(p,1),\ p = 0:(N-1)\} \cup \{(1,2s),\ s = 0:(N/2-1)\}.$$

$$\Phi_N = \{\arctan(1/p);\ p = 0:(N-1)\} \cup \{\arctan(2s);\ s = 0:(N/2-1)\}$$

Example: (p, s)=(1,2) **(arctan(2)=63.4349°)**

$$T_{1,2} = \{(0,0),(1,2),(2,4),(3,6),(4,8),(5,10),(6,12),(7,14),(8,0),(9,2),(10,4),(11,6),(12,8),(13,10),(14,12),(15,14)\}.$$

Replacement: $(p,s) \to (2k+1)(p,s),\quad k \in \{1,2,3,\ldots 7\}.$

$(p,s) = (1,2) \to (p,s) = (9,2)$ **(arctan(2/9)=12.5288°)**

$$T_{9,2} = \{(0,0),(9,2),(2,4),(11,6),(4,8),(13,10),(6,12),(15,14),(8,0),(1,2),(10,4),(2,6),(12,8),(5,10),(14,12),(7,14)\}.$$

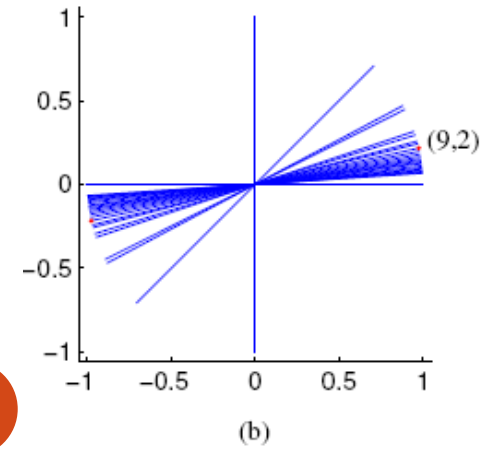

(b)

$J^1_{16,16}$

Generators and angles for (2k + 1)(p, s)-projections, when (p, s) = (1, 2).

$(2k+1)(p,s)$	$(1,2)$	$(3,6)$	$(5,10)$	$(7,14)$	$(9,2)$	$(11,6)$	$(13,10)$	$(15,14)$
$\varphi(k)$	63.43°	63.43°	63.43°	63.43°	12.52°	28.61°	37.56°	43.02°

Table 1. Generators and angles for $(2k+1)(p,s)$-projections, when $(p,s)=(1,2)$.

Equivalent sets of angles that are close to 45°, 60°, and 90°.

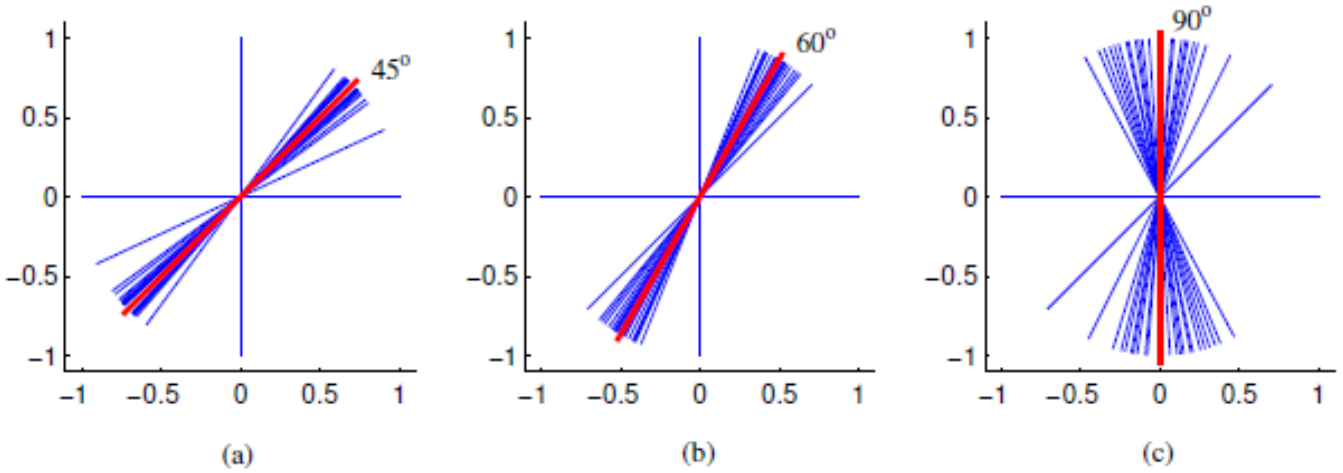

Figure 7. Sets of angles of projections at (a) 45˚, (b) 60˚, and (c) 90˚.

- Intersection between subsets $T_{p,s}$:

❑ (p,s)=(1,1) and (p,s)=(1,9)

$$T_{1,1} = \{(0,0), (1,1), (2,2), (3,3), (4,4), \ldots, (14,14), (15,15)\}$$

$$T_{1,9} = \{(0,0), (1,9), (2,2), (3,11), (4,4), \ldots, (14,14), (15,7)\}$$

❑ (p,s)=(1,2) and (p,s)=(1,10)

$$T_{1,2} = \{(0,0), (1,2), (2,4), (3,6), (4,8), \ldots, (14,12), (15,14)\}$$

$$T_{1,10} = \{(0,0), (1,10), (2,4), (3,14), (4,8), \ldots, (14,12), (15,6)\}$$

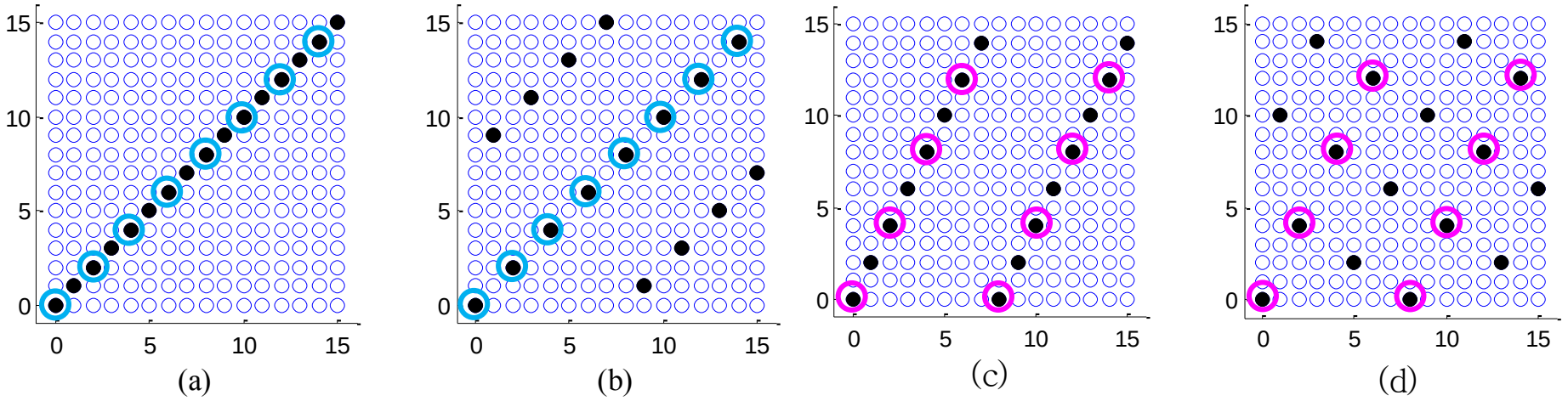

Figure 8. The covering of the 2-D DFT for (a) (1,1)-projection, (b) (1,9)-projection (c) (1,2)-projection, (d) (1,10)-projection

- Removal of the first 2 projections and 5 projections

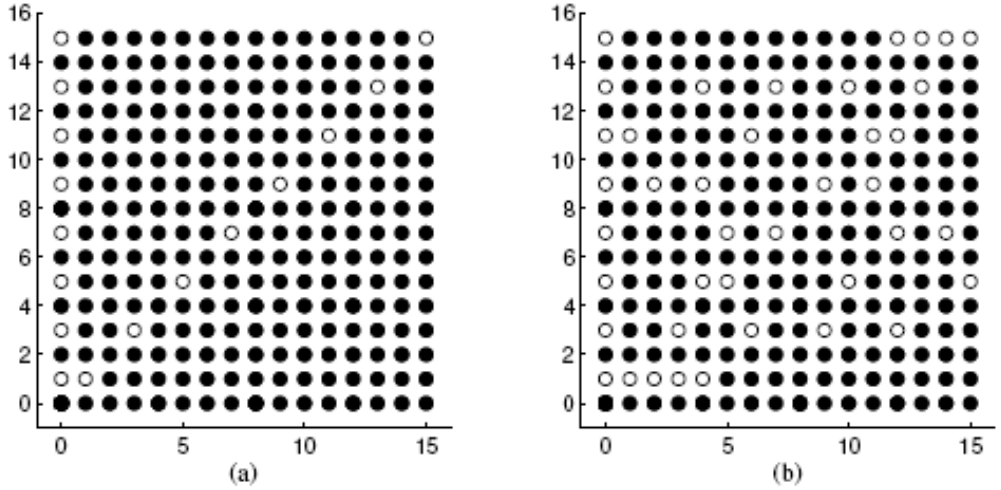

Grids in frequency domain

- Cartesian lattice and polar grid

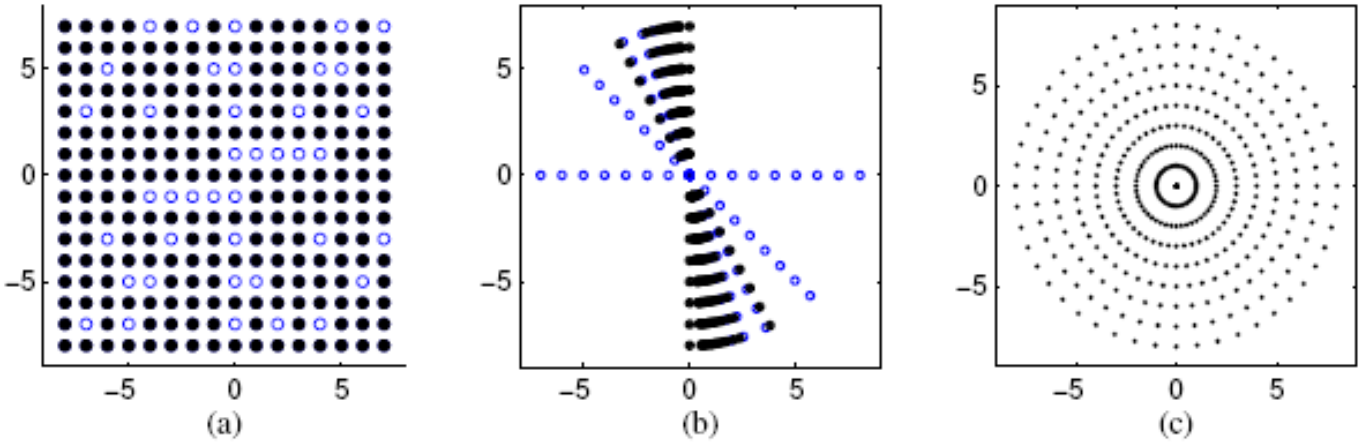

Ray-integrals and Ray-sums

- **Example :** Image reconstruction on the lattice 8×8.

I. (p, s)=(2,1)-projection

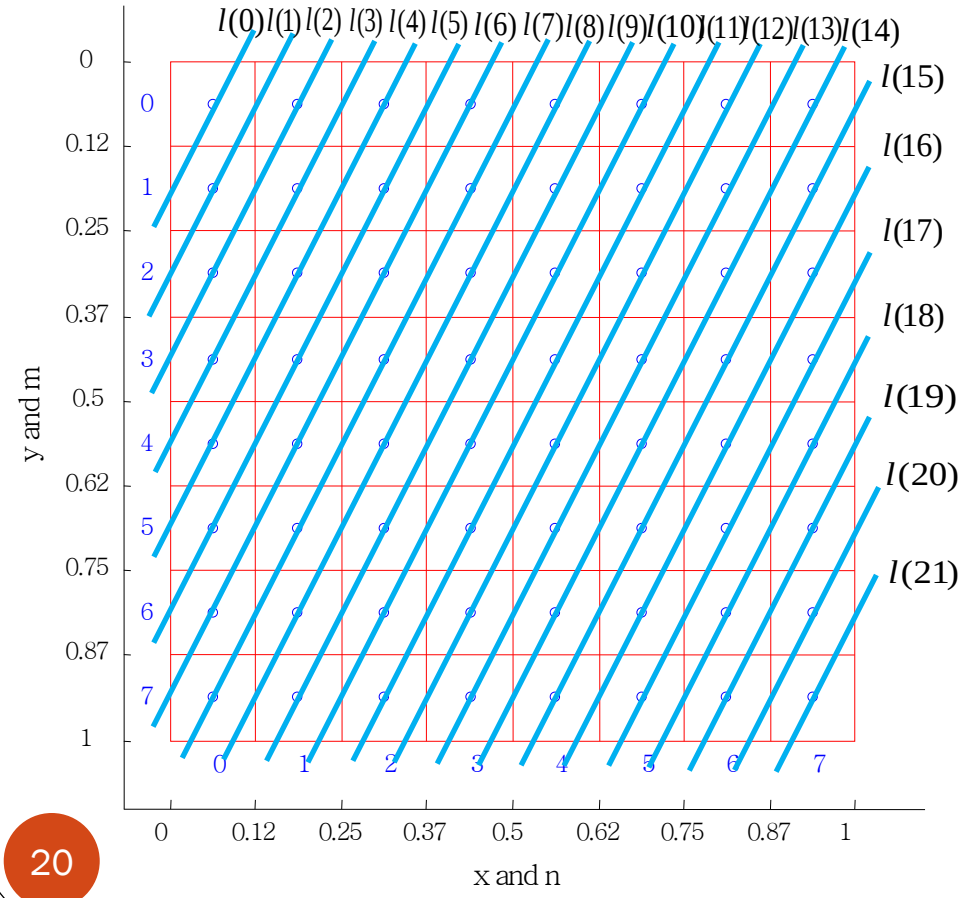

Rays of this projection:

$$l_{2,1}(t) = \{(x, y);\ 2x + y = \frac{t}{8} + \frac{3}{16}\}, \quad t = 0:21.$$

Ray-sums: $v_t = \sum_{(n,m)\in l} f_{n,m}, \quad t = 0:21$

Splitting-signal calculation:

$$f_{2,1,0} = v_0 + v_8 + v_{16}$$
$$f_{2,1,1} = v_1 + v_9 + v_{17}$$
$$f_{2,1,2} = v_2 + v_{10} + v_{18}$$
$$f_{2,1,3} = v_3 + v_{11} + v_{19}$$
$$f_{2,1,4} = v_4 + v_{12} + v_{20}$$
$$f_{2,1,5} = v_5 + v_{13} + v_{21}$$
$$f_{2,1,6} = v_6 + v_{14}$$
$$f_{2,1,7} = v_7 + v_{15}$$

I. (p, s)=(2,1)-projection

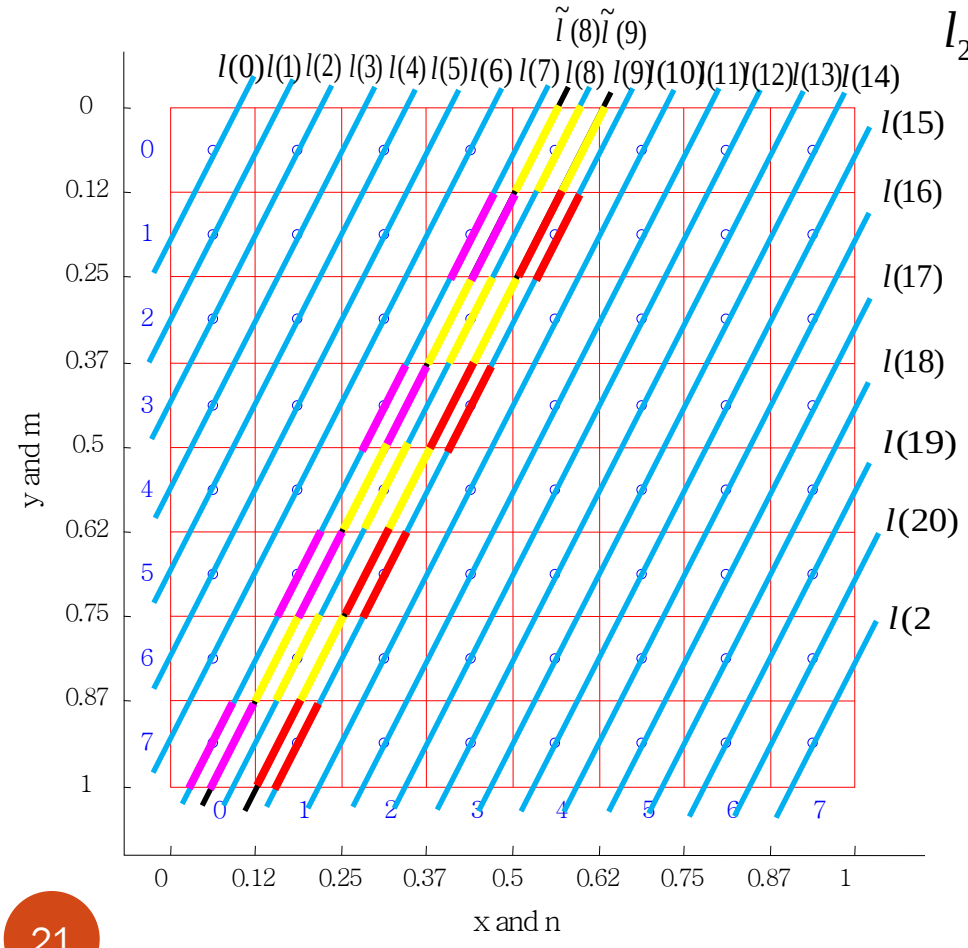

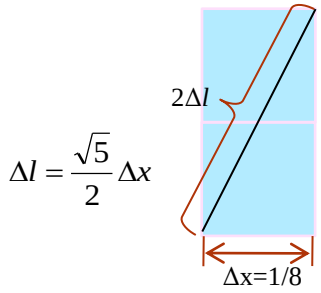

Geometrical Rays

$$l_{2,1}(t-0.5)=\{(x,y);\,2x+y=\frac{t}{8}+\frac{1}{8}\},\quad t=0:21.$$

Line-integrals:

$$w(8)=w(\tilde{l}(8))=8\sqrt{5}/2[v(7)+v(8)]$$

$$w(9)=w(\tilde{l}(9))=8\sqrt{5}/2[v(8)+v(9)]$$

Matrix form: $(8\sqrt{5}/2)Av=w$

$$\frac{8\sqrt{5}}{2}\begin{bmatrix}1&0&0&0&0&\dots&0&0&0\\1&1&0&0&0&\dots&0&0&0\\0&1&1&0&0&\dots&0&0&0\\0&0&1&1&0&\dots&0&0&0\\\dots&\dots&\dots&\dots&\dots&\dots&\dots&\dots&\dots\\0&0&0&0&0&\dots&1&1&0\\0&0&0&0&0&\dots&0&1&1\end{bmatrix}\begin{bmatrix}v(0)\\v(1)\\v(2)\\v(3)\\\vdots\\v(20)\\v(21)\end{bmatrix}=\begin{bmatrix}w(0)\\w(1)\\w(2)\\w(3)\\\vdots\\w(20)\\w(21)\end{bmatrix}$$

I. (p, s)=(2,1)-projection

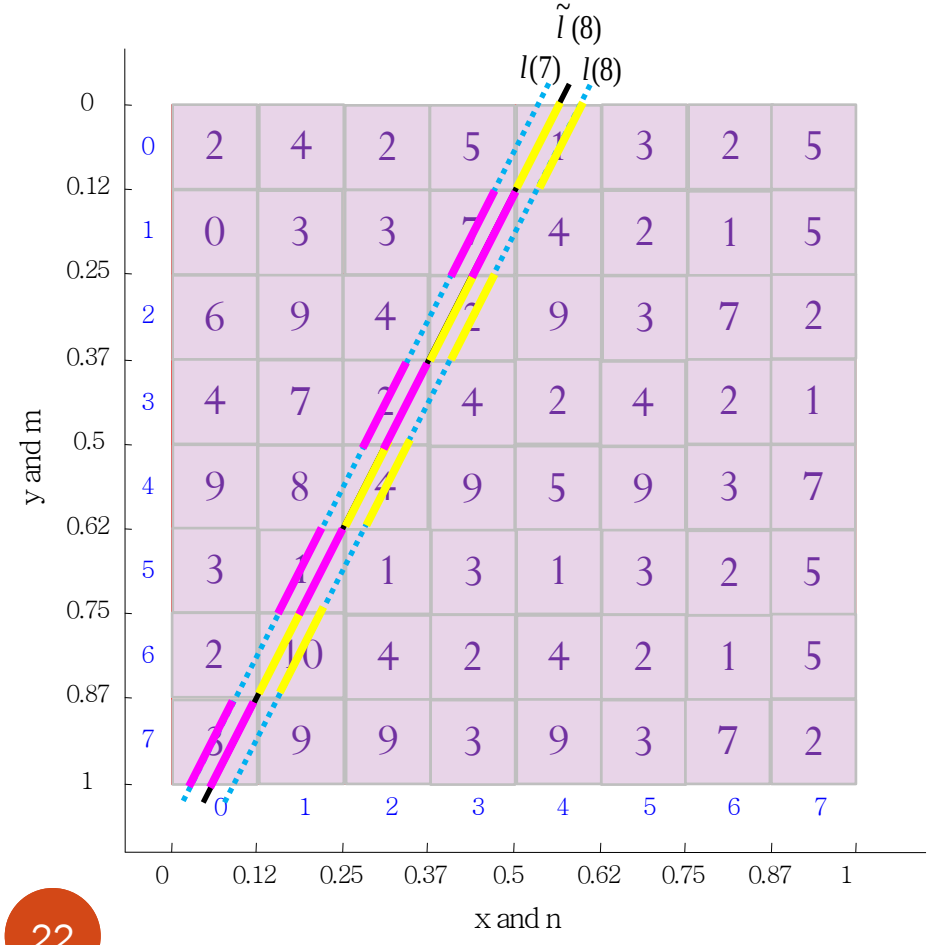

Line-integrals:

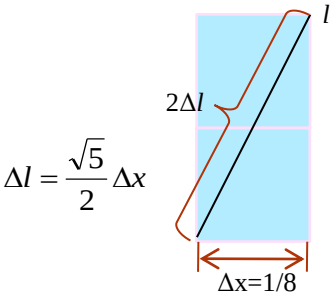

$$w(8) = w(\tilde{l}(8)) = w_l^{(4,0)} + w_l^{(3,1)} + w_l^{(3,2)} + w_l^{(2,3)} + w_l^{(2,4)} + w_l^{(1,5)} + w_l^{(1,6)} + w_l^{(0,7)}.$$

$$w_l^{(4,0)} = (\Delta l)\frac{f_{4,0}}{(\Delta x)^2} = (\Delta l)\frac{1}{(\Delta x)^2}$$

$$w_l^{(3,1)} = (\Delta l)\frac{f_{3,1}}{(\Delta x)^2} = (\Delta l)\frac{7}{(\Delta x)^2}$$

$$w_l^{(3,2)} = (\Delta l)\frac{f_{3,2}}{(\Delta x)^2} = (\Delta l)\frac{2}{(\Delta x)^2}$$

$$w_l^{(2,3)} = (\Delta l)\frac{f_{2,3}}{(\Delta x)^2} = (\Delta l)\frac{2}{(\Delta x)^2}$$

$$w_l^{(2,4)} = (\Delta l)\frac{f_{2,4}}{(\Delta x)^2} = (\Delta l)\frac{4}{(\Delta x)^2}$$

$$w_l^{(1,5)} = (\Delta l)\frac{f_{1,5}}{(\Delta x)^2} = (\Delta l)\frac{1}{(\Delta x)^2}$$

$$w_l^{(1,6)} = (\Delta l)\frac{f_{1,6}}{(\Delta x)^2} = (\Delta l)\frac{10}{(\Delta x)^2}$$

$$w_l^{(0,7)} = (\Delta l)\frac{f_{0,7}}{(\Delta x)^2} = (\Delta l)\frac{3}{(\Delta x)^2}$$

$$\frac{(\Delta l)}{(\Delta x)^2}(1+2+4+10) = \frac{(\Delta l)}{(\Delta x)^2}v(8), \quad v(8)$$

$$\frac{(\Delta l)}{(\Delta x)^2}(7+2+1+3) = \frac{(\Delta l)}{(\Delta x)^2}v(7), \quad v(7)$$

$$w(8) = \frac{8\sqrt{5}}{2}[v(7)+v(8)]$$

I. (p, s)=(2,1)-projection

Matrix form: $v = (2/8\sqrt{5})A^{-1}w$ $\Rightarrow$ $b = A^{-1}w$ $v_t = \frac{8\sqrt{5}}{2} b_t$

$$\begin{bmatrix} v(0) \\ v(1) \\ v(2) \\ v(3) \\ \vdots \\ v(20) \\ v(21) \end{bmatrix} = \begin{bmatrix} b(0) \\ b(1) \\ b(2) \\ b(3) \\ \vdots \\ b(20) \\ b(21) \end{bmatrix} \frac{2}{8\sqrt{5}} = \underbrace{\begin{bmatrix} 1 & 0 & 0 & 0 & \dots & 0 & 0 & 0 \\ -1 & 1 & 0 & 0 & \dots & 0 & 0 & 0 \\ 1 & -1 & 1 & 0 & \dots & 0 & 0 & 0 \\ -1 & 1 & -1 & 1 & \dots & 0 & 0 & 0 \\ \dots & \dots & \dots & \dots & \dots & \dots & \dots & \dots \\ 1 & -1 & 1 & -1 & \dots & -1 & 1 & 0 \\ -1 & 1 & -1 & 1 & \dots & 1 & -1 & 1 \end{bmatrix}}_{A^{-1}} \begin{bmatrix} w(0) \\ w(1) \\ w(2) \\ w(3) \\ \vdots \\ w(20) \\ w(21) \end{bmatrix}$$

Recursive form:

$$b_0 = w(0),$$
$$b_1 = w(1) - b_0,$$
$$b_2 = w(2) - b_1,$$
$$b_t = w(t) - b_{t-1}, \quad t = 3,4,\dots 21$$

Preliminary Results

Limited-angle range image reconstruction (Tensor transform)

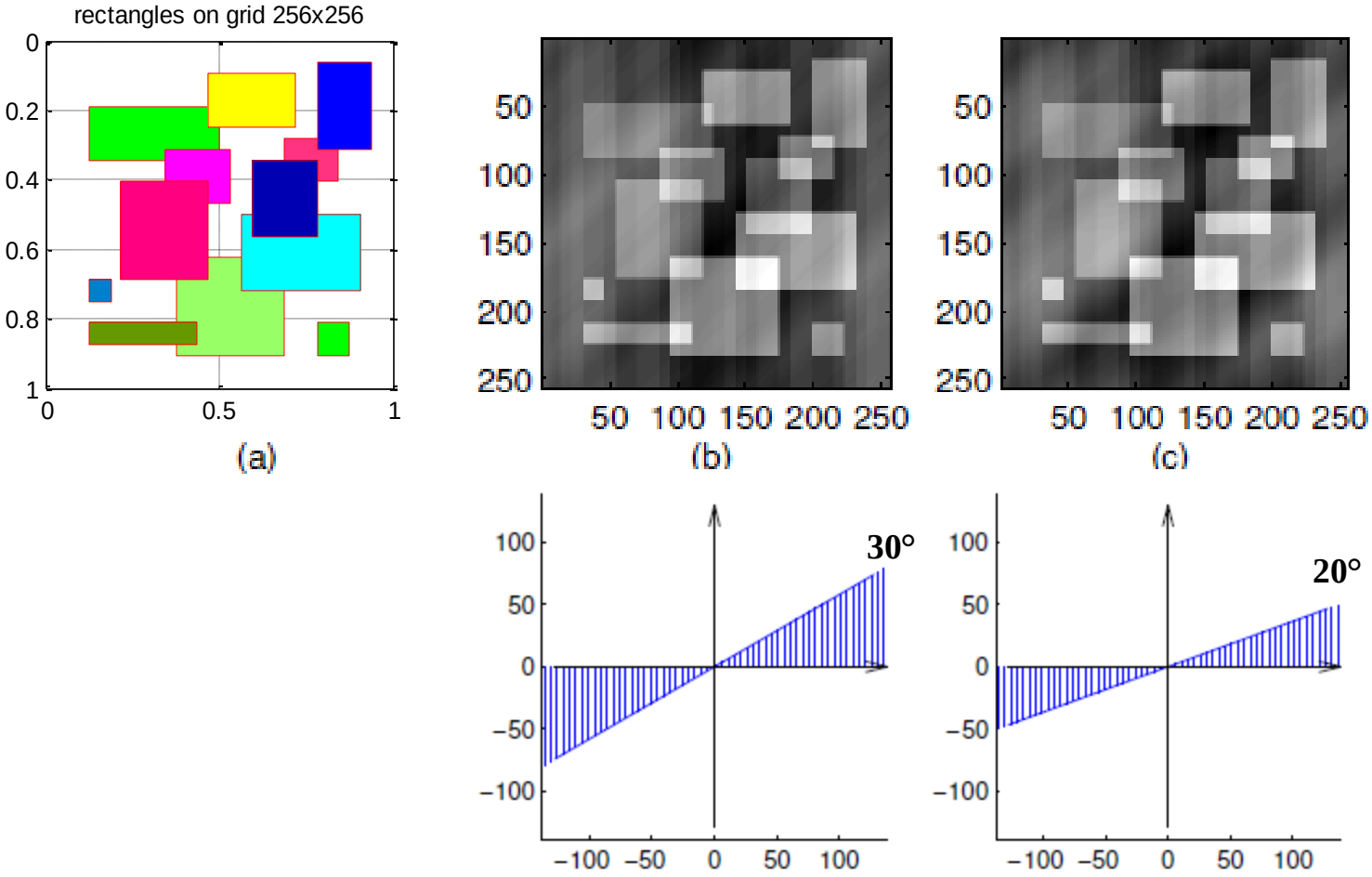

Figure 9. Original image on the lattice 256×256, and reconstruction by projections with the angles within the range of (b) [0, 30˚) and (c) [0, 20˚).

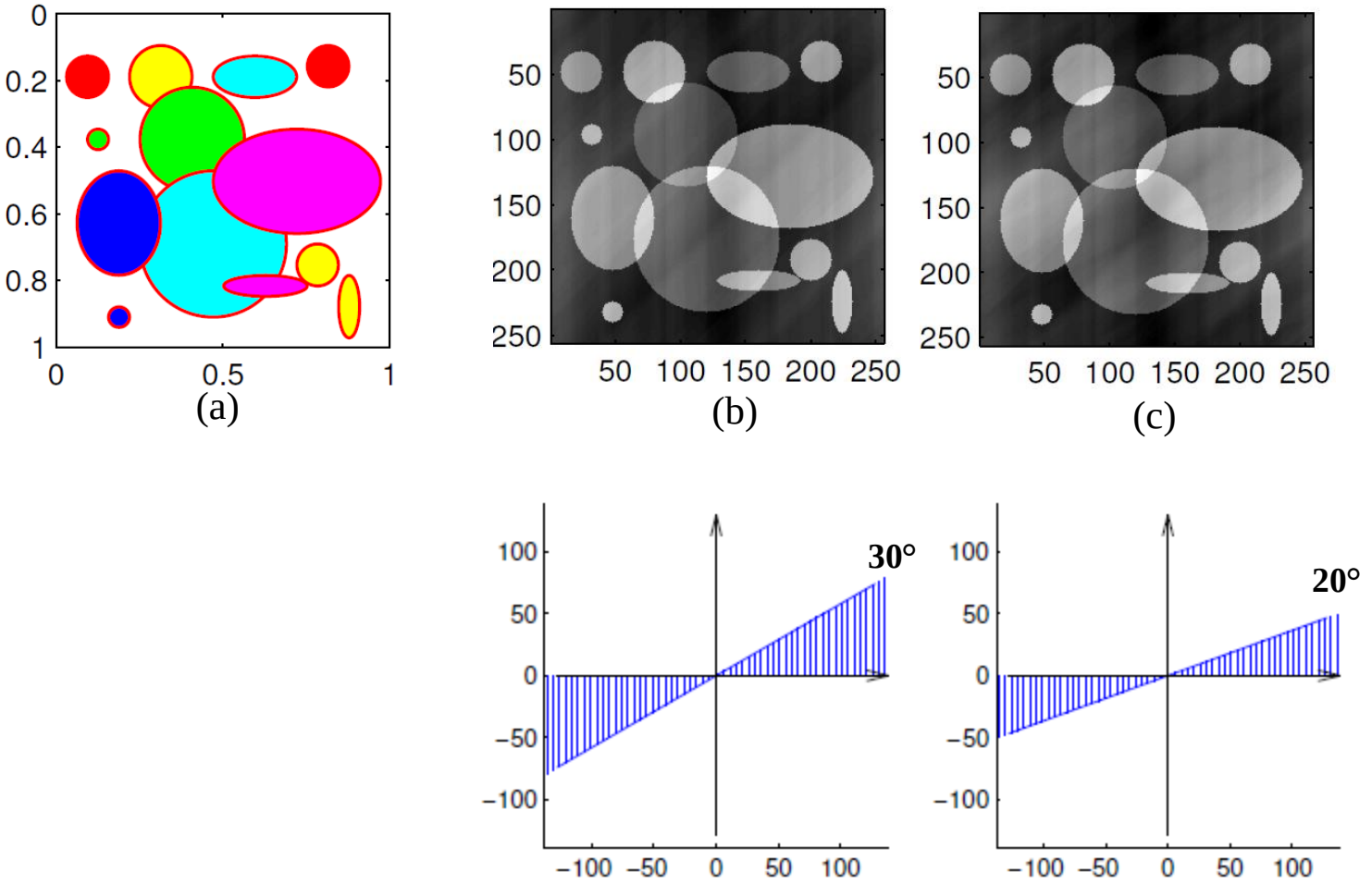

Figure 10. Original image on the lattice 256×256, and reconstruction by projections with the angles within the range of (b) [0, 30°) and (c) [0, 20°).

Comparison with Projections onto Convex sets (POCS) method

- Projection onto Convex sets (POCS)
  - known as alternating projection method
  - Iterative algorithm.

$$f_{i+1} = (P_m P_{m-1} \cdots P_1) f_i, \quad i = 1,2,3,\ldots$$

  - Relax algorithm

M.I.Sezan and H.Stark, "Tomographic image reconstruction from incomplete view data by convex projections and direct Fourier method."

$$\hat{f}_{i+1} = (T_5 T_2 T_3 T_1) \hat{f}_i, \quad i = 1,2,3,\ldots \qquad T_m = 1 + \lambda_m (P_m - 1)$$

relaxation parameter

- Projection operators
  - Projection P_1

$$P_1\hat{f} = g, \quad g_{n,m} = \begin{cases} \hat{f}_{n,m}, & \text{if } (n,m) \in A \\ 0\ , & \text{otherwise} \end{cases}$$

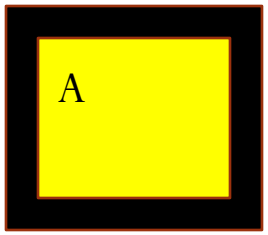

A={(n, m); 8≤n,m≤248}

  - Projection P_2

$$P_2\hat{f} = g, \quad G_{p,s} = \begin{cases} F_{p,s}, & \text{if } (p,s) \in L, \\ \hat{F}_{p,s}, & \text{otherwise.} \end{cases}$$

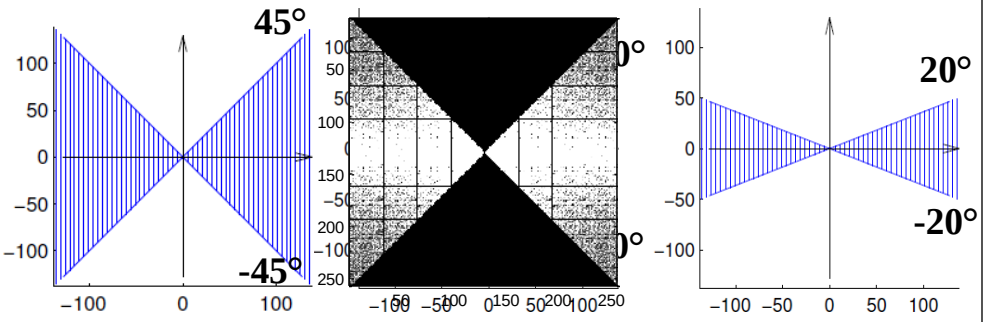

  - Projection P_3

$$P_3\hat{f} = \begin{cases} 0 & , \text{if } \hat{f} < 0, \\ \hat{f} & , \text{if } \hat{f} \geq 0,\ E[\hat{f}] \leq E_u, \\ (\sqrt{E_u / E[\hat{f}]})\,\hat{f} & , \text{if } \hat{f} \geq 0,\ E[\hat{f}] > E_u. \end{cases}$$

$$E[\hat{f}] = \sum_{n=0}^{N-1}\sum_{m=0}^{N-1}\left(\hat{f}_{n,m}\right)^2, \qquad E_u = E[f]$$

  - Projection P_5

$$P_5\hat{f} = g, \quad g_{n,m} = \begin{cases} a\ , & \text{if } \hat{f}_{n,m} < a, \\ \hat{f}_{n,m}\ , & \text{if } a \leq \hat{f}_{n,m} \leq b, \\ b\ , & \text{if } \hat{f}_{n,m} > b. \end{cases}$$

[a,b]=[0,1]

Comparison

Limited-angle range image reconstruction (by POCS):
Angle range: [−45°, 45°]

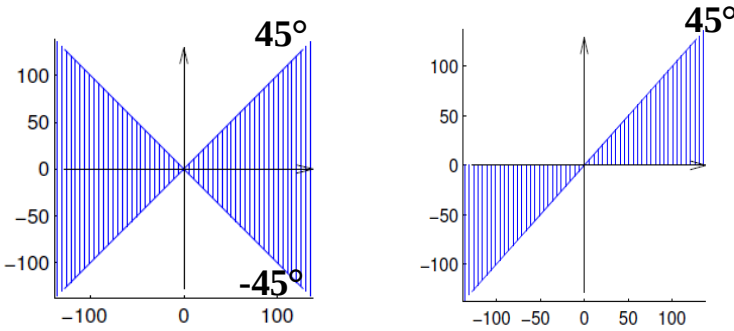

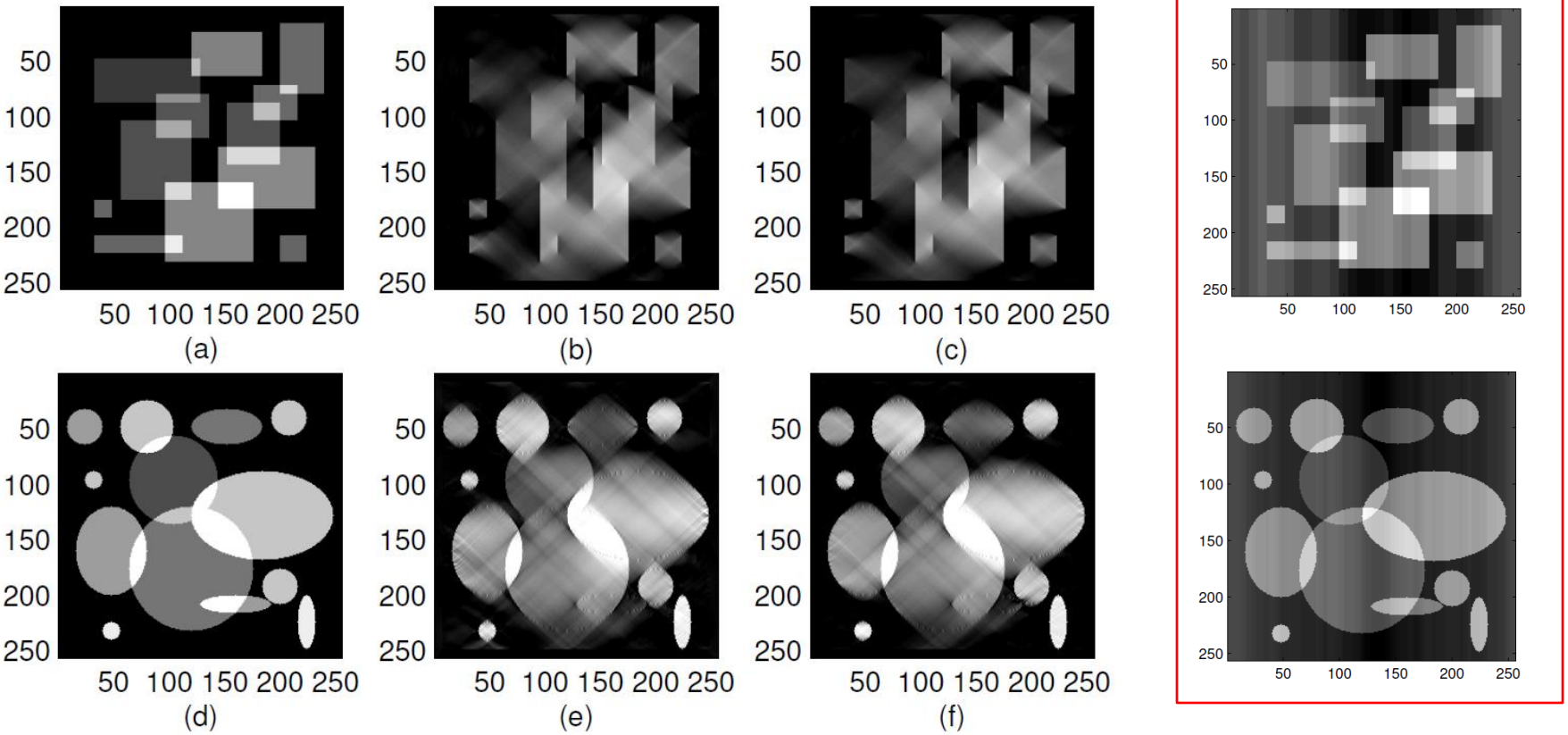

Figure 11. (a,d) Original images and reconstructions by the POCS algorithm, when the projection data are limited to [−45°, 45°] after (b,e) 30 and (c,f) 300 iterations.

Comparison

Angle range: [−30°, 30°]

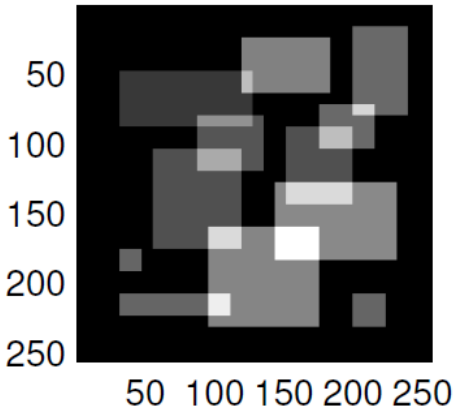

(a)

POCS

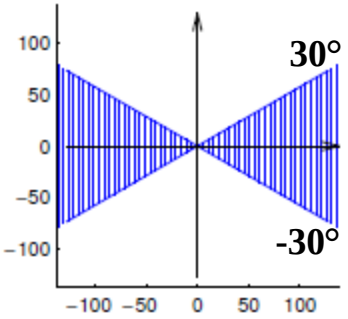

Tensor

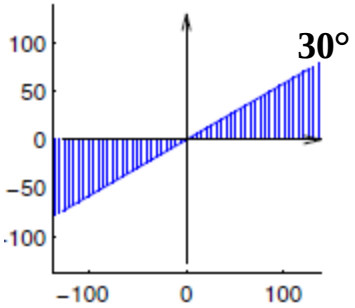

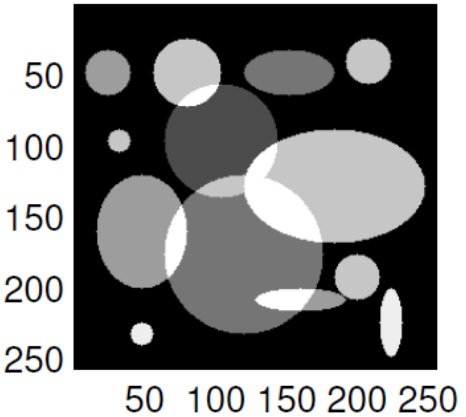

(d)

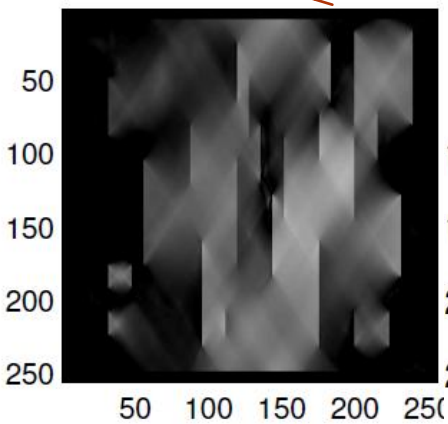

(b)

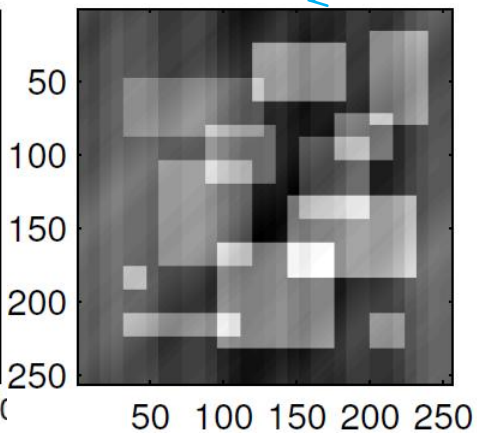

(c)

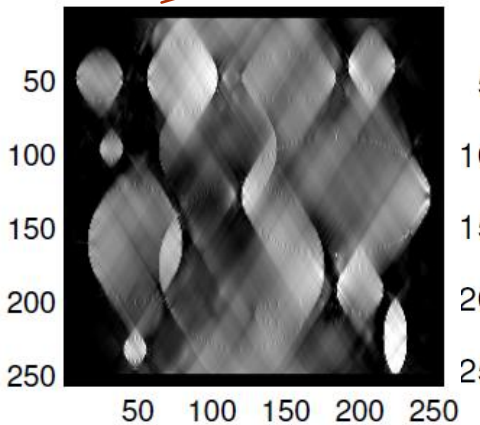

(e)

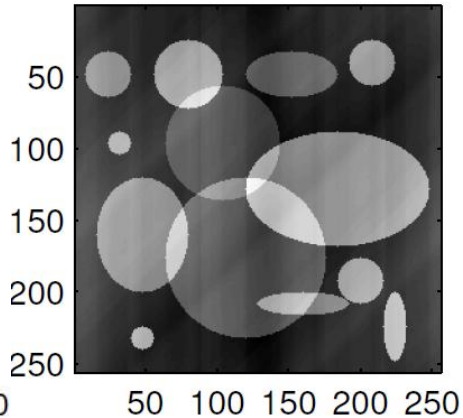

(f)

Comparison

Angle range: [−20°, 20°]

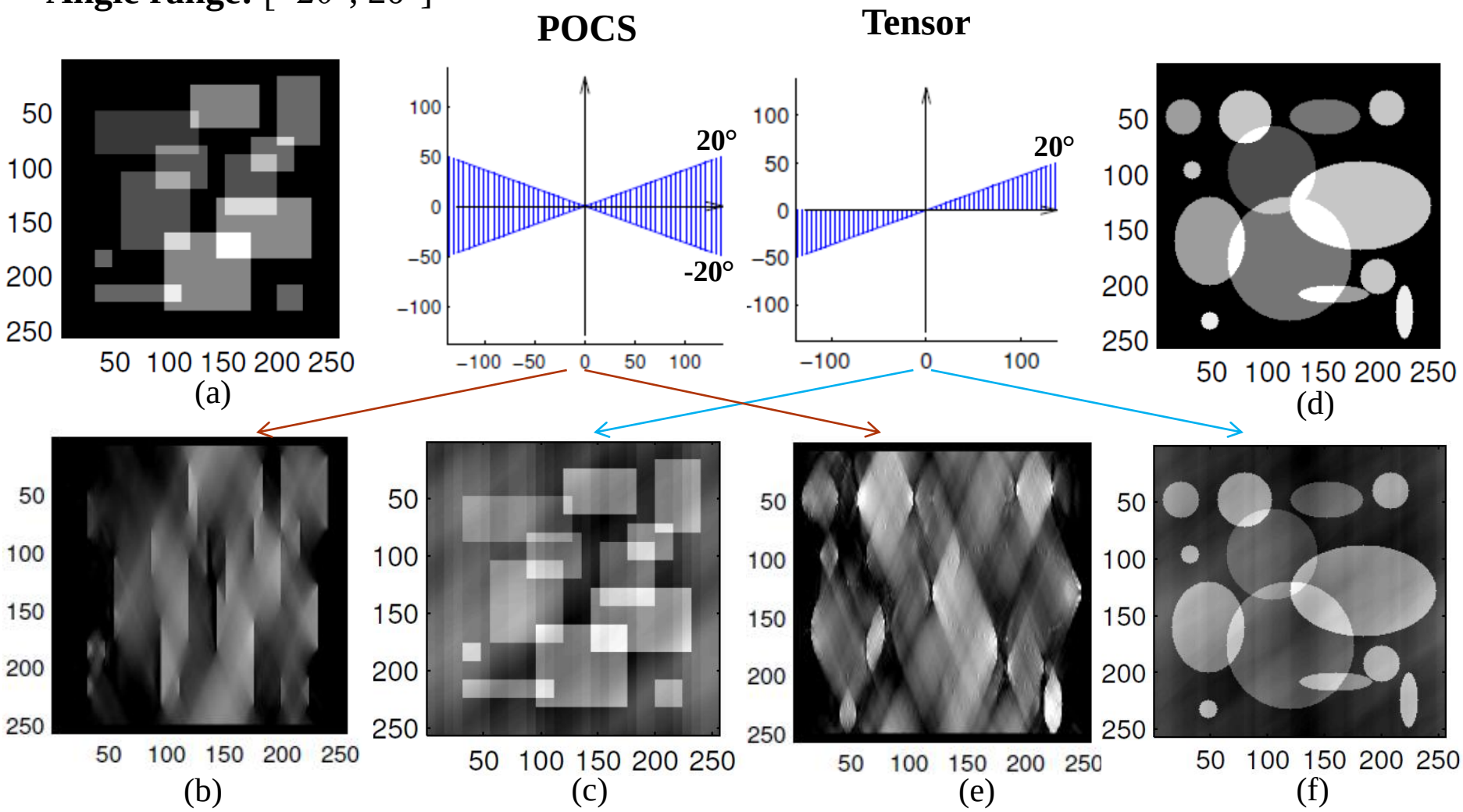

Noise Effect

- Noise of the projection data
  - Follows approximately a Gaussian distribution
  - Additive Gaussian noise with a distribution $N(0,\sigma^2)$
  - Signal independent

- Quantitatively Evaluation

  Reconstruction signal-to-noise ratio (SNR)

$$SNR = 10\log_{10}\frac{\sum_{n=0}^{N-1}\sum_{m=0}^{N-1}(f_{n,m})^2}{\sum_{n=0}^{N-1}\sum_{m=0}^{N-1}(\hat{f}_{n,m}-f_{n,m})^2}$$

$f_{n,m}$: Reference image- noise free Reconstruction

$\hat{f}_{n,m}$: Noisy Reconstruction

- Image reconstructions from limited angular range ([0,30°)) projections with Gaussian noise with mean 0

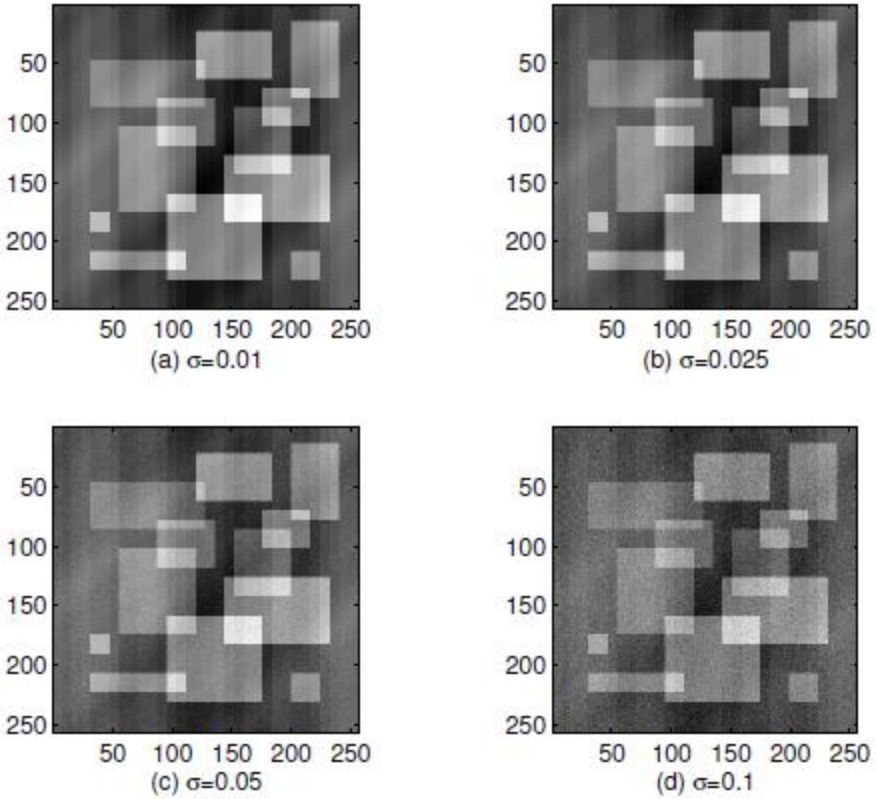

Figure 11. Image reconstructions from limited angular range projections with Gaussian noise with mean 0 and standard deviation (a) 0.01, (b) 0.025, (c) 0.05, and (d) 0.1.

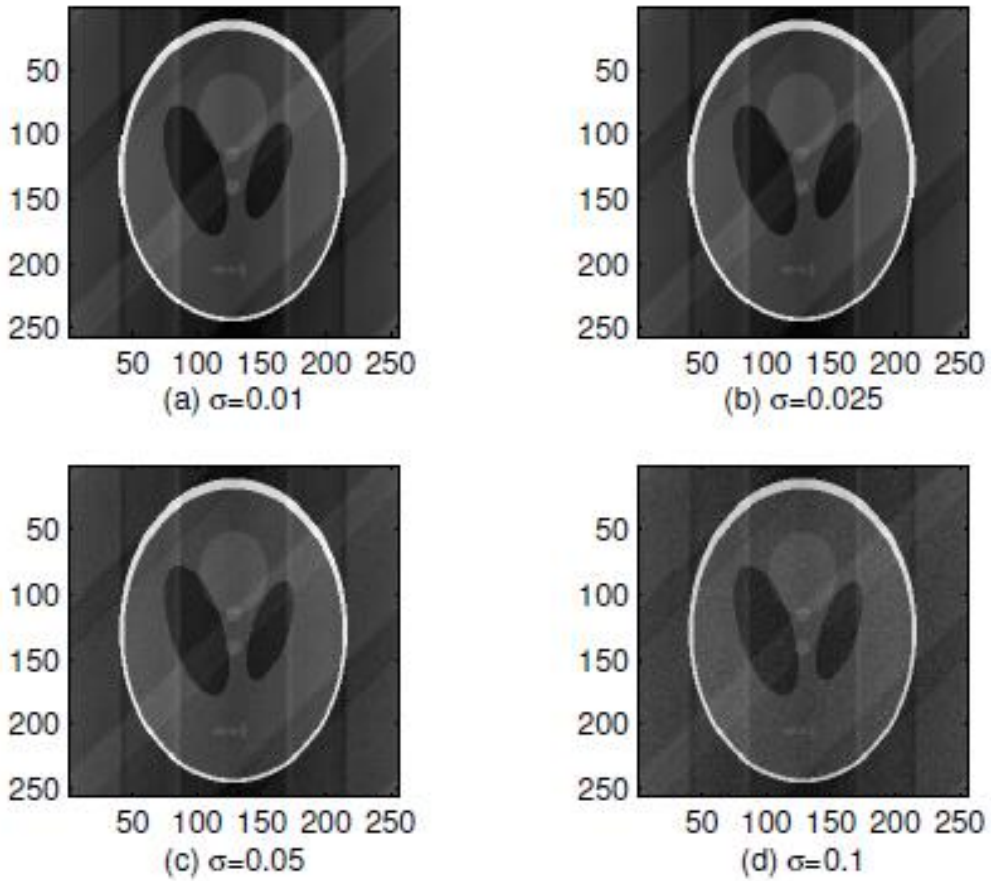

Figure 12. Phantom mage reconstructions from limited angular range projections with Gaussian noise with mean 0 and standard deviation (a) 0.01, (b) 0.025, (c) 0.05, and (d) 0.1.

Conclusion

A novel approach for reconstructing the discrete image on the Cartesian lattice from a finite number of projections of the image is applied. This approach is based on the tensor transform and an idea of transferring the geometry of integrals from the image space to the Cartesian lattice. All line-integrals over $f(x,y)$ image can be used for exactly calculating line-sums of the discrete image $f_{n,m}$ defined in the Cartesian lattice and the tensor transform of the image as the sum of direction images. The parallel beam scanning scheme is described and the reconstruction is exact.

Preliminary results show good results of image reconstruction when the angular range is 30° and down to 20°. The proposed method is also analyzed for the noisy projection data. The preliminary results show that the proposed method of reconstruction is robust relative to an additive signal-independent noise.

References

- [1] G.T. Herman, Image Reconstruction From Projections, New York: Academic Press, 1979.
- [2] D. E. Olins, A. L. Olins, H. A. Levy, R. C Durfee, S. M. Margle, E. P. Tinnel, and S. D. Dover, "Electron microscope tomography: Transcription in three dimensions," Science, vol. 220, pp. 498–500, 1983.
- [3] A.C. Kak and M. Slaney, Principles of Computerized Tomographic Imaging, IEEE Press, New York, 1987.
- [4] A.M. Grigoryan and M.M. Grigoryan, Image Processing: Tensor Transform and Discrete Tomography with MATLAB, CRC Press Taylor and Francis Group, Boca Raton, 2012.
- [5] A.M. Grigoryan and Nan Du, "Principle of superposition by direction images," IEEE Trans. on Image Processing, vol. 20, no. 9, pp. 2531–2541, September 2011.
- [6] A.M. Grigoryan and S.S. Agaian, Multidimensional Discrete Unitary Transforms: Representation, Partitioning, and Algorithms, New York: Marcel Dekker, 2003.
- [7] A.M. Grigoryan and M.M. Grigoryan, Brief Notes in Advanced DSP: Fourier Analysis With MATLAB, CRC Press Taylor and Francis Group, 2009.
- [8] A.M. Grigoryan, "Image reconstruction from finite number of projections: Method of transferring geometry," IEEE Trans. on Image Processing, vol. 22, no. 12, pp. 4738–4751, December 2013.
- [9] M.I. Sezan and H. Stark, "Tomographic image reconstruction from incomplete view data by convex projections and direct Fourier method," IEEE Trans. Med. Imaging, vol. MI-3, pp. 91–98, June. 1984.
- [10] D.C. Youla and H. Webb, "Image Restoration by the Method of Convex Projections: Part 1–Theory," IEEE Trans. Med. Imaging, vol. MI-1, pp. 81–94, Oct. 1982.
- [11] M.I. Sezan and H. Stark, "Image restoration by the method of projections onto convex sets, Part 2–Applications and numerical results," IEEE Trans. Med. Imaging, vol. MI-1, pp. 95–101, Oct. 1982.
- [12] O. Demirkaya, "Reduction of noise and image artifacts in computed tomography by nonlinear filtration of the projection images," Proc. SPIE Med. Imaging, vol. 4322, pp. 917–923, 2001.
- [13] H. Lu, I.-T. Hsiao, X. Li, and Z. Liang, "Noise properties of low-dose CT projections and noise treatment by scale transformations," Proc. IEEE Nucl. Sci. Symp, vol. 3, pp. 1662–1666, Nov. 2001.

THANK YOU VERY MUCH!

QUESTIONS, PLEASE?